

# UPSIDE

Deliverable D2.2

Grant Agreement No.	101070931
Start date of Project	1 September 2022
Duration of the Project	48 months
Choose an item.	<b>D2.2: Conformable IGT-array (1500 interfacescm<sup>2</sup> ) with superior SNR (20 dB increase) and 1 month in vitro stability</b>
Partner Leader	UG
Dissemination Level	PU


<i>Status</i>	Final
<i>Version</i>	V1.0
<i>Choose an item. Date</i>	30-09-2024

<i>Author(s)</i>	Sofia Drakopoulou (UG), Georgios Spyropoulos (UG)
<i>Co-author(s)</i>	

UPSIDE project has received funding from the European Union's Horizon Europe EIC-PATHFINDER programme under grant agreement No 101070931.




European  
Innovation  
Council



	Funded by the European Union. Views and opinions expressed are however those of the author(s) only and do not necessarily reflect those of the European Union or EISMEA. Neither the European Union nor the granting authority can be held responsible for them
---	---

PU=Public, SEN=Confidential, only for members of the consortium (including the Commission Services), CI=Classified, as referred to in Commission Decision 2001/844/EC.

## House Style

	Red RGB	Green RGB	Blue RGB	HEX
				
Pink	247	181	192	#F7B5C0
Grey	161	161	161	#A1A1A1
Blue	41	171	226	#29ABE2
 <p>THE USE OF THE EU EMBLEM IN THE CONTEXT OF EU PROGRAMMES 2021-2027 <a href="#">LINK</a>            In addition to the obligations set out in <a href="#">Article 17</a>, communication and dissemination activities as well as infrastructure, equipment or major results funded under EIC actions must also display the following special logo:</p>				
<p>European Innovation Council </p>				
EU corporate blue	0	51	153	#003399
Yellow	255	204	0	#FFCC00

## Authors, Co-authors and contributors

Author	Organization
Sofia Drakopoulou	UG
Georgios Spyropoulos	UG

## Quality Control

Author	Name	Date
WP leader	Georgios Spyropoulos	30-09-2024
Coordinator	Tiago Lopes Marta da Costa	30-09-2024

## History of Changes

Version	Change made	Date
V1.0		30-09-2024

## Table of Contents

Executive Summary.....	3
1. Introduction .....	4
2. Development of passive MEAs .....	5
2.1 Design and development of flexible IGT probes.....	5
2.2. In vitro characterization stability.....	9
3. Conclusions .....	11

## List of Figures:

Figure 2-1: Microscope images showcasing the step-by-step fabrication of IGT arrays for parameter optimization and microfabrication techniques. A) Photoresist patterning. B) Gold traces with parylene insulation. C) Deposition of channels and ion membrane over gold tracks to form the transistor, with labelled Source (S), Gate (G), and Drain (D).....	5
Figure 2-2: Output characteristics of an IGT with very high transconductance (120mS) and ms range temporal response.....	5
Figure 2-3: Two front-end designs of 1st generation IGT-based probes employing IGTs with $L=1\mu\text{m}$ , $L=2\mu\text{m}$ and $W/L$ ratios 5,10. ....	7
Figure 2-4: Microscope image of a flexible ion-gated transistor (IGT) probe after the lift-off process of the Au layer.....	7
Figure 2-5: A) Illustration of transistor use in neural recordings, comparing passive and active electrodes. "N" represents biological noise, "S" is the neurophysiological signal, and "Nline" refers to line noise. The terms "aS," "aN," and "Nline" denote the amplified signals. B) Sample ECG traces: Red: Recorded using an e-IGT interface, with a peak-to-peak signal of 1.7 mA and RMS noise of 3.1 $\mu\text{A}$ (SNR = 55 dB). Blue: Recorded using a commercially available medical TENS electrode, with a peak-to-peak signal of 1.1 mV and RMS noise of 19 $\mu\text{V}$ (SNR = 35 dB). ....	8
Figure 2-6: Left column: Output characteristics ( $I_D - V_D$ ) of IGT device ( $L = 5 \mu\text{m}$ , $W = 50 \mu\text{m}$ ) for gate voltage ( $V_G$ ) varying from 0 V (top curve) to +0.6 V (bottom curve) with a step of +0.1 V for Day 1 and Day 35; color intensity corresponds to $V_G$ amplitude. Right column: Transfer curves for $V_D = -0.6\text{V}$ (black ) and the corresponding transconductance (orange).....	9
Figure 2-7: Maximum transconductance ( $g_{m,max}$ ) of IGTs measured over 35 day period of time.....	10
Figure 2-8: Normalized temporal response of IGTs measured over a 35-day period of time.....	10

## Executive Summary

This work highlights the development of conformable transistor arrays based on internal ion-gated organic electrochemical transistors (IGTs). By optimizing design and microfabrication, we achieved high and stable gain-bandwidth product. The arrays demonstrated in vitro stability over a month, as well as high signal-to-noise ratio (SNR) during biological data acquisition. These key features make the IGT arrays highly suitable for integration into neural probes. The deliverable was completed on time, with no delays or impact on other project milestones or objectives.

UNDER REVIEW

## 1. Introduction

The objectives of WP2 consisted of : (i) Development of conformable polymer-based passive MEAs with ultra-low impedance; (ii) Development of IGT-arrays for on spot amplification of neurophysiological signals.

UNDER REVIEW

## 2. Development of passive MEAs

In Task 2.2 (Development of IGT-arrays), UG has developed and microfabricated ion-gated organic electrochemical transistor (IGT) arrays. The goal is to optimize these arrays and integrate them into neural probes to efficiently record electrophysiological signals with a high SNR (Task 2.3: Intra-operative animal-model neurophysiological recordings). The optimization process for these IGT arrays was broken down into several steps to identify the best methods for fabrication, connections, and design specifications like size and shape.

### 2.1 Design and development of flexible IGT probes

At the earlier stage of Task 2.2., we have designed and microfabricated a range of ion-gated transistor (IGT) arrays to refine the microfabrication steps and evaluate how the dimensions of these arrays influence their transconductance and temporal response. These factors are essential for achieving a high signal-to-noise ratio during electrophysiological recordings. Initially, we developed photolithography masks incorporating IGT arrays with various channel widths and lengths (Figure 2.1).

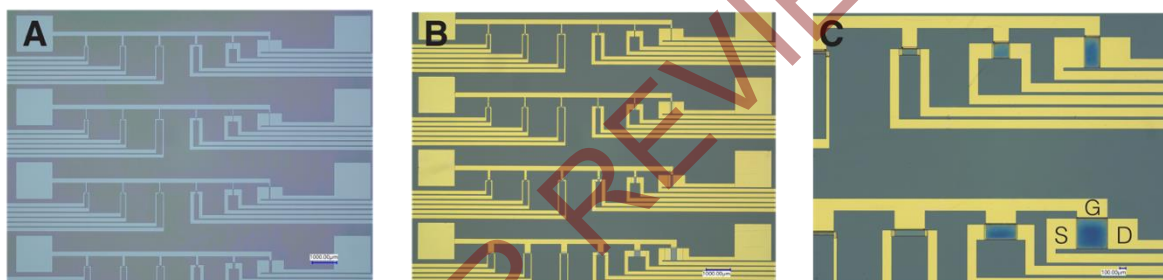


Figure 2-1: Microscope images showcasing the step-by-step fabrication of IGT arrays for parameter optimization and microfabrication techniques. A) Photoresist patterning. B) Gold traces with parylene insulation. C) Deposition of channels and ion membrane over gold tracks to form the transistor, with labelled Source (S), Gate (G), and Drain (D).

These designs were specifically tailored for on-bench testing, allowing connection with Source Measurement Units (SMUs) and micro-positioners. During these tests we were able to show transistors with very high transconductance values (120mS) and ms range temporal response (Figure 2.2).

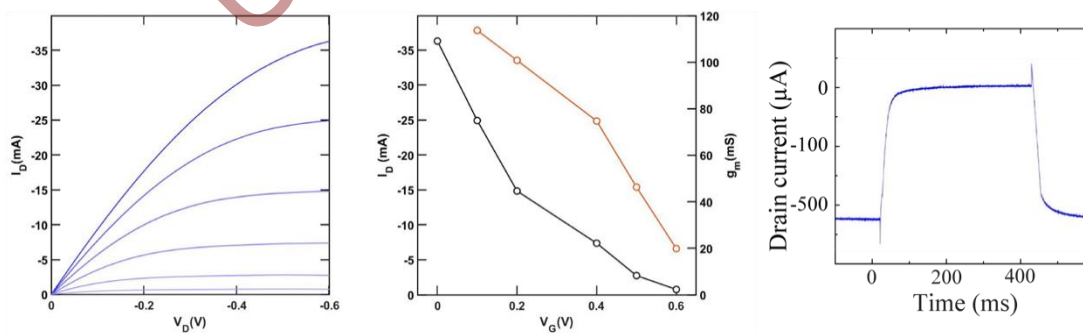


Figure 2-2: Output characteristics of an IGT with very high transconductance (120mS) and ms range temporal response.

All data from analysis and feedback from the microfabrication processes were gathered to design and develop the first-generation, fully IGT-based flexible probe, advancing toward their use in practical applications. Two distinct front-end designs were developed and fabricated, each integrating IGTs optimized for high gain-bandwidth products (i.e., high transconductance and fast temporal response).

- i) A linear array of IGT transistors designed for implantation in the brain or to achieve linear cortical coverage. The interface area for this design, which includes 8 channels, measures approximately  $150\ \mu\text{m} \times 250\ \mu\text{m}$ .
- ii) An IGT transistor array designed for coordinated spatial resolution of the cortex, featuring 16 channels and an interface area of approximately  $250\ \mu\text{m} \times 350\ \mu\text{m}$ .

Both probe designs feature transistors with short channel lengths ( $L = 1\ \mu\text{m}$  or  $L = 2\ \mu\text{m}$ ) and width-to-length ( $W/L$ ) ratios of 5 and 10. These compact spatial characteristics enable a high gain-bandwidth product while maintaining a minimal interface footprint ( $\sim 10\ \mu\text{m}^2$ ), comparable to the size of individual neurons (**Figure 2.3**). As a result, our probes achieve a high interface density, exceeding 1600 interfaces per  $\text{cm}^2$ .

Like previous electrode array designs, the IGT-based probes utilize a back-end with BGA-like contacts to enable flip-chip bonding and eventual integration with a CMOS recording interface. The interconnection ribbons have been thoughtfully engineered to maximize flexibility and ease of use, without sacrificing performance, drawing on prior experience and insights from discussions with UF. These ribbons are approximately 3 cm in length, with a progressively decreasing footprint for each interconnection. To enhance placement and handling, all front-end designs include an anchor hole that facilitates precise micromovements and simplifies array implantation.

UNDER REVIEW

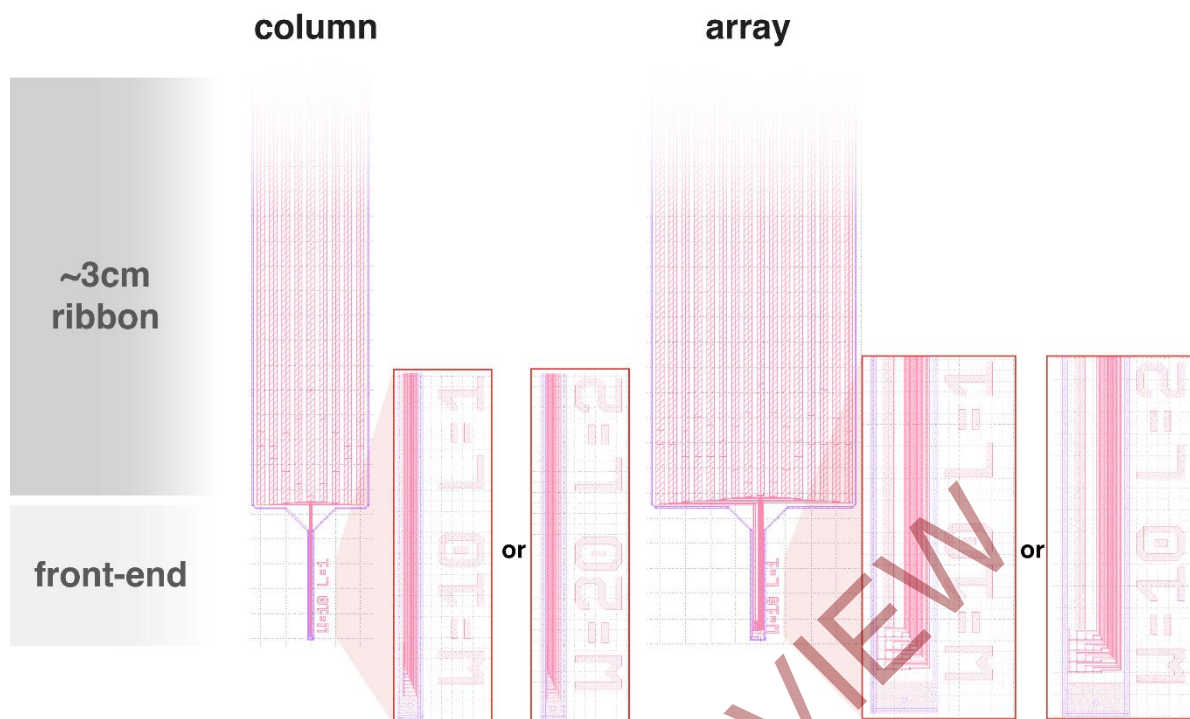


Figure 2-3: Two front-end designs of 1st generation IGT-based probes employing IGTs with  $L=1\mu\text{m}$ ,  $L=2\mu\text{m}$  and  $W/L$  ratios 5,10.

**Figure 2.4** presents microscope images of two representative probes following the Au layer lift-off process. The upper image displays a linear array with 8 transistor interfaces, each featuring a channel length of  $L = 2\mu\text{m}$  and a  $W/L$  ratio of 10. The lower image shows an array with 16 transistor interfaces, all with a channel length of  $L = 2\mu\text{m}$  and a  $W/L$  ratio of 5. In both designs, the transistors share a common source, while each drain electrode has a separate interconnection. For in vitro characterization, an Ag/AgCl electrode will function as the gate, whereas in vivo, the biological events themselves will serve this role.

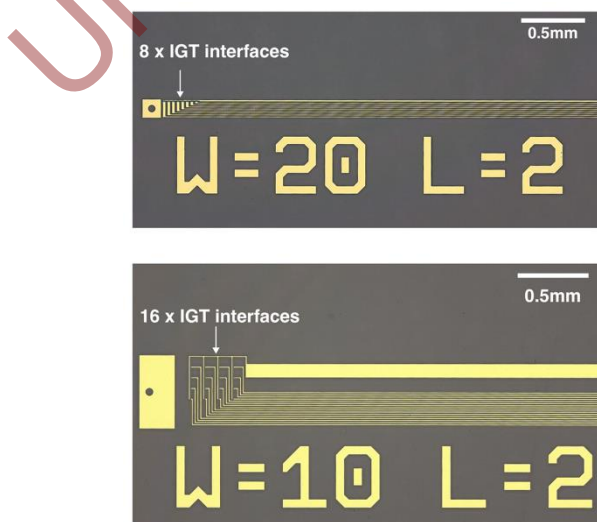


Figure 2-4: Microscope image of a flexible ion-gated transistor (IGT) probe after the lift-off process of the Au layer.



IGTs offer a significantly higher signal-to-noise ratio (SNR) compared to conventional electrodes, even those with similar or larger surface areas. This advantage stems from the ability of IGTs to provide on-site amplification, which eliminates the need to amplify the noise from interconnection lines (**Figure 2.5A**)—a common issue in dense arrays. In such arrays, the smaller, more resistive interconnection footprints lead to increased noise. **Figure 2.5B** compares ECG traces recorded with an IGT interface ( $L = 50 \mu\text{m}$ ,  $W = 100 \mu\text{m}$ ) to those from commercially available TENS electrodes, which have a much larger footprint ( $L = 4 \text{ cm}$ ,  $W = 8 \text{ cm}$ ). The IGTs achieved an SNR of approximately 55 dB, whereas the TENS electrodes exhibited an SNR of around 35 dB.

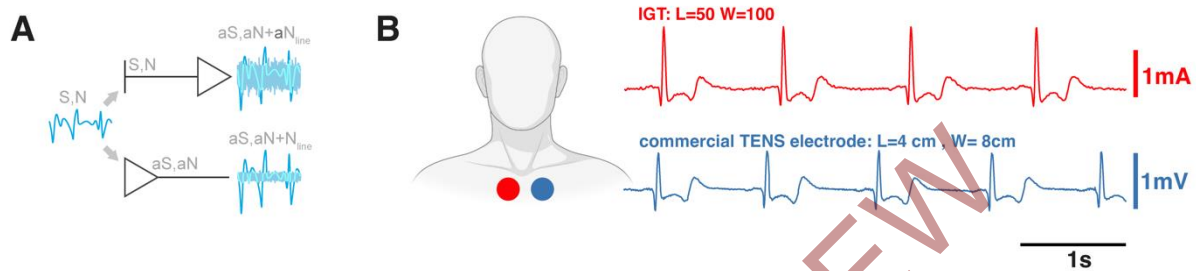


Figure 2-5: A) Illustration of transistor use in neural recordings, comparing passive and active electrodes. "N" represents biological noise, "S" is the neurophysiological signal, and "Nline" refers to line noise. The terms "aS," "aN," and "Nline" denote the amplified signals. B) Sample ECG traces: Red: Recorded using an e-IGT interface, with a peak-to-peak signal of 1.7 mA and RMS noise of  $3.1 \mu\text{A}$  (SNR = 55 dB). Blue: Recorded using a commercially available medical TENS electrode, with a peak-to-peak signal of 1.1 mV and RMS noise of  $19 \mu\text{V}$  (SNR = 35 dB).

UNDER REVIEW

## 2.2. In vitro characterization stability

To evaluate the in vitro stability and performance of IGTs, we measured their steady-state and temporal characteristics over a period of 35 days. To simulate in vivo conditions, the IGTs were immersed in Phosphate-Buffered Saline (PBS) solution and stored at room temperature for the whole duration of the experiment. Weekly measurements were conducted to assess whether the IGTs maintained consistent performance parameters, such as transconductance and temporal response.

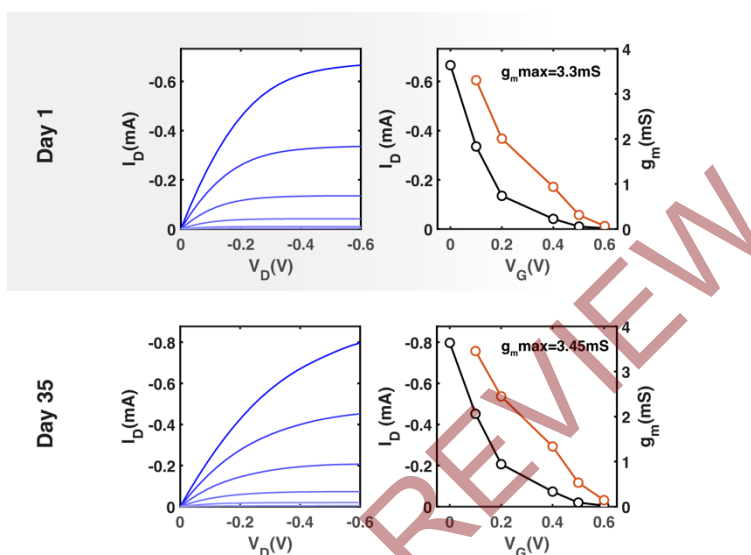


Figure 2-6: Left column: Output characteristics ( $I_D - V_D$ ) of IGT device ( $L = 5 \mu\text{m}$ ,  $W = 50 \mu\text{m}$ ) for gate voltage ( $V_G$ ) varying from 0 V (top curve) to +0.6 V (bottom curve) with a step of +0.1 V for Day 1 and Day 35; color intensity corresponds to  $V_G$  amplitude. Right column: Transfer curves for  $V_D = -0.6\text{V}$  (black) and the corresponding transconductance (orange).

The IGT operated in depletion mode, meaning that when a positive gate voltage was applied, mobile ions from the ion reservoir near the PEDOT-rich regions of the film compensated the sulfonate anions on the PSS. This caused a reduction in the hole density within the PEDOT, leading to a decrease in channel current (**Figure 2.6**). From the corresponding transfer curves, we extracted the transconductance values. To assess the long-term performance and stability, we plotted the maximum transconductance ( $g_{m,\text{max}}$ ) over time. **Figure 2.7** illustrates the  $g_{m,\text{max}}$  derived from these IV curves, showing relatively stable values over a 35-day period. After the first 14 days, the maximum transconductance showed a slight increase, likely due to additional hydration of the channel, leading to a higher concentration of mobile ions and improved ion mobility near the PEDOT-rich regions. Following this initial rise,  $g_{m,\text{max}}$  showed a minor decline but remained consistently higher than the initial transconductance throughout the entire tested period. These results communicate stable performance over time.

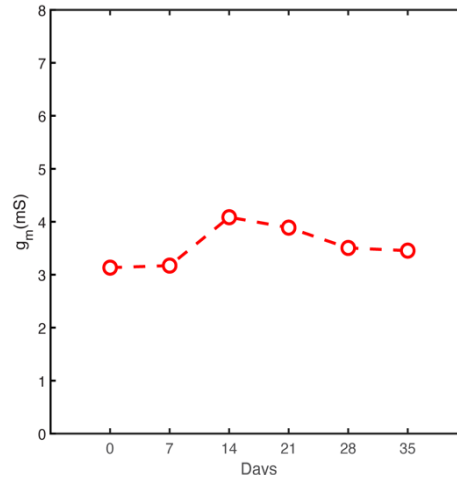


Figure 2-7: Maximum transconductance ( $g_{m,max}$ ) of IGTs measured over 35 day period of time.

To further evaluate stability, we monitored the temporal response ( $I$  vs  $t$ ) of the IGTs over the same 35-day period. **Figure 2.8** shows the normalized temporal response of the drain current ( $I_D$ ) over 35 days, with a drain voltage ( $V_D$ ) of  $-0.6V$  and a gate voltage ( $V_G$ ) pulse amplitude of  $0.6V$ . Similar to the trend observed in  $g_{m,max}$ , the amplitude of  $\Delta I$  modulation showed a slight increase during the first few days, followed by stabilization. This aligns with the findings from our  $g_{m,max}$  measurements, supporting the hypothesis that increased hydration and ion mobility in the channel influence the device's performance.

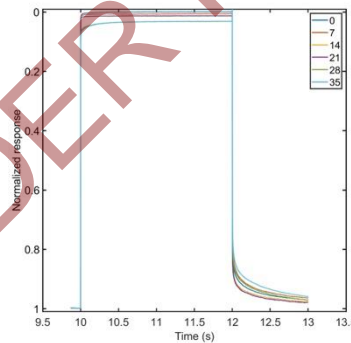


Figure 2-8: Normalized temporal response of IGTs measured over a 35-day period of time.

### 3. Conclusions

We have optimized the microfabrication processes to develop ion-gated organic electrochemical transistor (IGT) probes with a high interface density. Thanks to their compact spatial design (W, L), the IGTs demonstrated high transconductance ( $g_m$  max) at a gate voltage of 0V, and achieved a high signal-to-noise ratio (SNR) in electrophysiological signal acquisition, highlighting their strong performance in depletion mode. The arrays also maintained consistent temporal responses and exhibited good electrical stability under in vitro tested physiological conditions for a period of 35 days, making them well-suited for neural recording applications. With the successful completion of fabrication and initial characterization, the project remains on track for upcoming deliverables, including further validation and optimization for in vivo applications.

UNDER REVIEW